Dynamic Equilibrium Mechanism for Surface Nanobubble Stabilization

Michael P. Brenner[1] and Detlef Lohse[2]

[1]*School of Engineering and Applied Sciences, Harvard University, Cambridge, Massachusetts 02138, USA*
[2]*Physics of Fluids Group, Faculty of Science and Technology, MESA$^+$ and Impact Institutes, University of Twente,
7500 AE Enschede, The Netherlands*

Recent experiments have convincingly demonstrated the existence of surface nanobubbles on submerged hydrophobic surfaces. However, classical theory dictates that small gaseous bubbles quickly dissolve because their large Laplace pressure causes a diffusive outflux of gas. Here we suggest that the bubbles are stabilized by a continuous influx of gas near the contact line, due to the gas attraction towards hydrophobic walls [Dammer and Lohse, Phys. Rev. Lett. **96**, 206101 (2006); Zhang *et al.*, Phys. Rev. Lett. **98**, 136101 (2007); Mezger *et al.*, J. Chem. Phys. **128**, 244705 (2008)]. This influx balances the outflux and allows for a metastable equilibrium, which, however, vanishes in thermodynamic equilibrium. Our theory predicts the equilibrium radius of the surface nanobubbles, as well as the threshold for surface nanobubble formation as a function of hydrophobicity and gas concentration.

Various recent studies have revealed the existence of nanoscopic soft domains at the liquid-solid interface [1–16]. As atomic force microscopy (AFM) shows, these soft domains resemble spherical caps with heights of ≈ 10 nm and diameters of $2R \approx 100$ nm, corresponding to a small contact angle (on the gas side) of $\theta \approx 10°$, see Fig. 1 for a sketch. The most consistent interpretation [17] of these soft domains is that they are *surface nanobubbles*, i.e., nanoscale gas bubbles located at the liquid-solid interface. Spectroscopic studies [15,18] and x-ray reflectivity measurements [19–21] experimentally confirm the presence of gas at the wall. Moreover, the size and density of these objects depend on the dissolved gas concentration and they disappear completely when the liquid is degassed [10–12,18,22]. CO_2 bubbles have a much shorter lifetime (only 1–2 h) as compared to air bubbles, due to the much lower pressure of CO_2 in the atmosphere and its better solubility in water [15]. The existence of these surface nanobubbles has potentially great technological importance, as they have been shown to result in fluid slip in hydrophobic surfaces, leading to a potentially large reduction in fluid dissipation for flows in small devices [23–25].

Observations of long lived surface nanobubbles flatly contradicts the classical theory of bubble stability [26]. Small bubbles have large internal gas pressures, in order to balance the compressive action of surface tension. For a bubble in water of radius $R = 50$ nm, which with above contact angle $\theta = 10°$ corresponds to a radius of curvature $R_c = R/\sin\theta \approx 250$ nm, and surface tension $\gamma = 73$ mN/m (20° temperature), the gas pressure according to classical macroscopic theory (neglecting the disjoining pressure [27]) is $P_{\text{gas}} = 2\gamma/R_c = 2\gamma\sin\theta/R = 0.58$ MPa. In employing Laplace's equation we also neglect the bubble-stabilizing contribution from hydroxide ion adsorption on the bubble surface [28]. If the resulting charge density is

constant, this ion adsorption contributes a radius-independent term to P_{gas}, which is negligible for small enough bubbles. Henry's law then dictates that the concentration of gas at the bubble surface is $c(R) = c_0 P_{\text{gas}}/P_0$, where c_0 is the saturated concentration of gas at atmospheric pressure P_0. This is necessarily much larger than the gas concentration $c_\infty \leq c_0$ far away, leading to a diffusive outflux of gas and bubble dissolution [26,29]. *If* the contact angle θ remains finite for $R \rightarrow 0$ and assuming that Laplace's law remains valid at molecular scales, then $c(R)$ formally diverges, signaling the breakdown of the continuum approach.

Various suggestions have been made to explain the long lifetime of surface nanobubbles. Among these, the reduction of surface tension for large curvature on small scales
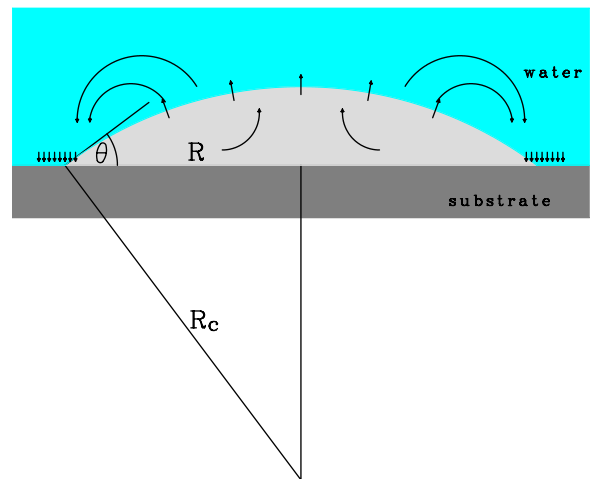

FIG. 1 (color online). Sketch of gas outflux and influx into a surface nanobubble and definition of the contact angle θ, the surface nanobubble radius R, and the radius of curvature R_c.

[30,31] (operative for bubbles smaller than ~ 5 nm), the oversaturation of the liquid around the nanobubbles with gas [7,15], the effect of induced charges in the Debye layer around the bubble interface [32], or the stabilization of bubbles due to contaminant molecules in the water [33], similarly as has been suggested for microbubbles in contaminated water [34]. In this Letter we propose an alternative mechanism for bubble stabilization, namely, that the gas outflux is compensated by gas influx at the contact line.

The diffusive mass outflux from a surface nanobubble is given by

$$J_{\text{out}}(R) = D \int dA\mathbf{n} \cdot \nabla c \approx 2\pi D \int_0^R rdr\partial_z c, \quad (1)$$

where D is the diffusion constant of gas in the liquid (typically 10^{-9} m^2/s) and $\mathbf{n}$ is the normal vector to the droplet surface. We have assumed that the bubble is nearly flat, so that the diffusive gradient is primarily in the $\hat{z}$ direction, perpendicular to the solid surface. This diffusive flux can then be evaluated by solving the steady state diffusion equation in the liquid. The result is

$$J_{\text{out}}(R) = \pi RD[c(R) - c_\infty] = \pi RD\left(\frac{c_0}{P_0}\frac{2\gamma\sin\theta}{R} - c_\infty\right). \quad (2)$$

The volume flux rate $j_{\text{out}}(R) = J_{\text{out}}(R)/c(R)$ is then given by

$$j_{\text{out}}(R) = \frac{J_{\text{out}}(R)}{c(R)} = \pi RD\left(1 - \frac{c_\infty}{c(R)}\right). \quad (3)$$

The volume of the bubble thus decreases linearly with time, typically with a volume flux rate $\approx \pi RD \approx \pi \times 50 \times 10^{-9} \times 10^{-9}$ m^3/s, when assuming complete degasing. For an initial bubble of radius 50 nm, this implies a dissolution timescale of ~ 1 μs.

Stabilization against dissolution requires a physical effect to cancel this diffusive outflux. Although intermolecular forces might modify the liquid surface tension from its macroscopic value [27,31], the energetic cost of creating surface energy ensures that the gas pressure in the bubble is always higher than that of the surrounding liquid, and hence diffusive outflux necessarily persists even when interactions with the solid surface are accounted for. Stabilization can be achieved however, by mechanisms causing an *influx* of gas into the bubble. Such an influx need not occur uniformly across the bubble surface, but can be spatially concentrated. In particular, it is quite natural to consider influx mechanisms near the contact line, where intermolecular forces are most significant. For a sketch of the gas flow directions, we refer to Fig. 1. The magnitude of any contact line dominated influx increases with the circumference of the bubble, and hence could compete effectively with the diffusion mediated outflux Eqs. (2) and (3).

What is the origin of such an influx? Recent MD simulations [35–37] of gas dissolved in water in contact with a surface demonstrated that on hydrophobic surfaces there is

gas enrichment near solid walls. Such an enhanced gas concentration at hydrophobic walls has been confirmed spectroscopically [15,16] and with x-ray reflectivity measurements [19–21]; also neutron reflectivity experiments [38] suggest it. In the MD simulations of Ref. [35], for sufficiently hydrophobic walls the concentration near walls can exceed more than 2 orders of magnitude above the concentration in bulk liquid. Physically, this enrichment occurs because there is a potential $\phi(z)$ attracting solute molecules to the wall. The equilibrium concentration of the solute is thus determined by the balance between diffusion and attraction, according to $D\frac{dc}{dz} = -\frac{1}{\zeta}\frac{d\phi}{dz}c$ where ζ is the mobility of the solute. The Einstein relation $D = k_BT/\zeta$ then implies the equilibrium distribution of solute as $c(z) = c_0\exp(-\phi(z)/k_BT)$. A hundredfold concentration of solute molecules near the wall as found for the case studied in Ref. [35] implies that $\phi(z)$ decreases by about $4k_BT$ near the wall, over a molecularly determined length scale. In general, we assume that the energy gain $\Delta\phi$ of a solute molecule at the wall equals $\Delta\phi = sk_BT$.

Solute molecules at a gas-liquid interface are attracted to the wall and hence driven inside the bubble; see again Fig. 1. The size of the gas influx J_{in} is given by

$$J_{\text{in}}(R) \approx 2\pi \int_0^R rdrc(r)\frac{1}{\zeta}\frac{d\phi(z = h(r))}{dz}. \quad (4)$$

Here we have again approximated the bubble shape $h(r)$ as nearly flat. Since the attractive force drops off quickly with distance, the flux is only appreciable near the contact line. Using the fact that near the contact line $h(r) = (R - r) \times \tan\theta$ we can approximate Eq. (4) to obtain the mass influx $J_{\text{in}}(R) \approx 2\pi Rc(R)\Delta\phi/(\zeta\tan\theta)$, or the volume influx

$$j_{\text{in}}(R) = \frac{J_{\text{in}}(R)}{c(R)} \approx \frac{2\pi sDR}{\tan\theta}. \quad (5)$$

As anticipated above, Eq. (5) suggests that the influx scales linearly with R, exactly the same scaling as the diffusive outflux. However, recent measurements [39–42], including some on surface nanobubbles [43,44], have shown that for sufficiently small bubbles or droplets, the contact angle θ depends on the contact line curvature and thus on the bubble size, i.e., $\theta = \theta(R)$. This can be described through a modified Young-Dupré equation

$$\cos(\pi - \theta) = \cos(\pi - \theta_\infty) - \frac{C}{R + \delta}, \quad (6)$$

where C and δ are constants with the dimensions of length, and θ_∞ is the usual macroscopic equilibrium contact angle. A popular (though disputed [39]) model assumes that the correction arises from a line tension τ of the contact line [45], in which case $C = \tau/\gamma$, where γ is the liquid surface tension. The ratio C/δ is set by the contact angle θ_0 for $R \to 0$, namely $C/\delta = \cos(\pi - \theta_\infty) - \cos(\pi - \theta_0)$, so that one can rewrite (6) as

$$\cos\theta = \cos\theta_\infty - \frac{\cos\theta_\infty - \cos\theta_0}{1 + R/\delta}. \quad (7)$$

The length scale δ is the onset scale of microscopic corrections to the macroscopic contact angle. The exact form of Eq. (7) and the exact values of the parameters are not relevant in the context of this Letter; all that is needed is that $\theta(R)$ decreases with decreasing bubble radius R, which indeed is observed in Refs. [39,40,43,44]. We take $\delta = 70$ nm, $\theta_\infty = 50°$, and $\theta_0 = 0°$. Note that the behavior $\theta(R \to 0) = 0$ leads to a stabilization of small surface nanobubbles, as their curvature becomes small. In the limiting case $R \to 0$ it even vanishes and the numerically found [35] case of a mono- or bilayer of gas molecules between the surface and the liquid is recovered.

The outflux $j_{\text{out}}(R)$ and the influx $j_{\text{in}}(R)$ are shown in Fig. 2 for some typical parameters. In that case, a *stable* dynamic equilibrium radius R^* defined through $j_{\text{out}}(R^*) = j_{\text{in}}(R^*)$ exists. Note that indeed various studies have revealed the existence of a *preferred* radius of the surface nanobubbles [6,15], which depends on the gas concentration [15]. For bubbles smaller than the equilibrium radius, the influx overcompensates the outflux, for larger bubble the outflux wins. If the gas concentration c_∞ decreases, the outflux increases and the equilibrium radius is becoming smaller, in agreement with experimental observations on nanobubbles [12]. If, on the other hand, the surface gets more hydrophobic and θ_∞ decreases and/or the attraction potential s increases, the equilibrium radius is shifted towards larger values, again in agreement with experimental observations.

The necessary condition for a stable dynamic equilibrium and therefore for stable nanobubbles to exist is that at small bubble sizes $R \to 0$ the influx $j_{\text{in}}(R)$ is larger than the
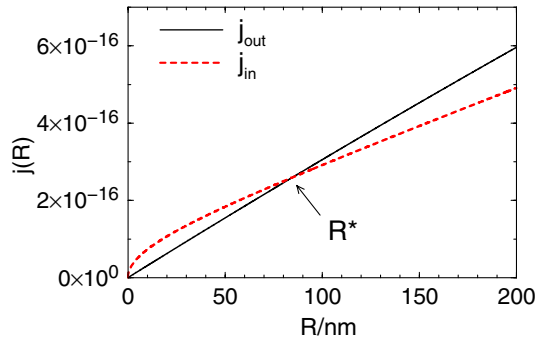
FIG. 2 (color online). Gas outflux j_{out} [black-solid line, from Eq. (3)] and influx j_{in} [red-dashed line, from Eq. (5)] into the surface nanobubble as function of bubble radius R. The crossing point defines the equilibrium radius R^*. The units of j are m^3/s. If the slope of j_{out} at $R = 0$ is larger than that of j_{in}, no surface nanobubbles can emerge. For this illustrative plot we used Eq. (7) with $\delta = 70$ nm, $\theta_\infty = 50°$, and $\theta_0 = 0°$, and the values $s = 0.36$ for the relative strength of the attraction potential, $c_\infty/c_0 = 0.25$ for the relative gas concentration, and $D = 10^{-9}$ m²/s (which only scales the y axis). For these data the stable equilibrium radius is $R^* = 85$ nm.

outflux $j_{\text{out}}(R)$. This implies the condition

$$s > \frac{1}{2}\tan\theta_0\left(1 - \frac{c_\infty}{c(R \to 0)}\right) \approx \frac{1}{2}\tan\theta_0 \quad (8)$$

for small gas concentration $c_\infty \ll c(R \to 0)$. The condition (8) is satisfied for sufficiently hydrophobic surfaces, where $\tan[\theta(R \to 0)]$ is small enough and when the solute is attracted to the wall, so that s is large enough. If condition (8) is fulfilled, there also is an unstable equilibrium at $R^* = 0$, allowing for spontaneous nanobubble formation. If that condition is not fulfilled, the equilibrium at $R^* = 0$ becomes stable and no surface nanobubbles form, in spite of an enhanced gas concentration very close to the surface. These may have been the conditions of the X-ray reflectivity experiments of Ref. [19], where a gas accumulation, but no nanobubbles, have been seen.

How does the preferred bubble radius R^* depend on the material properties and the control parameters? To illustrate this dependence, we show $R^*(s, c_\infty/c_0)$ resulting from our simple model [Eqs. (3), (5), and (7), see Fig. 3]. The dependence of R^* on the attraction strength s is as expected rather strong—slight (chemical or structural) inhomogeneities in the surface will therefore result into some distribution in the preferred radius, as indeed experimentally seen in Refs. [6,15]. In contrast, away from saturation, the dependence on the exact value of the relative gas concentration c_∞/c_0 is relatively weak.

Some comments on the driving mechanism: While the gas diffuses in the liquid, there is a gas flow from the contact line towards the surface inside the bubble. To avoid conflict with the second law of thermodynamics, such a state can only be transient. We do not know the origin of the nonequilibrium; it could be caused by temperature gradients, chemical effects, or local oversaturation. In principle the observation method itself (e.g., AFM or optical detection of the nanobubbles) could be the origin of the equilibrium distortion. If the system were isolated, the second law of thermodynamics requires that in the long term (possibly hours or even days) the driving mechanism would expire and the surface nanobubbles therefore dis-
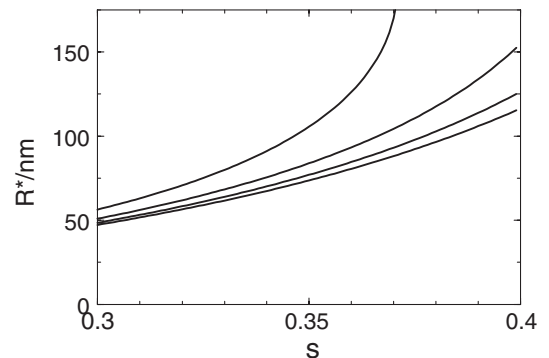
FIG. 3. Dependence of equilibrium radius R^* on the wall attraction strength s for relative gas concentrations $c_\infty/c_0 = 0.1, 0.25, 0.5, 0.95$, bottom to top.

solve, i.e., nanobubbles would be a transient phenomenon. Unfortunately, long-term observations of surface nanobubbles in closed systems have to our knowledge not yet been carried out. Note that the required nonequilibrium situation must also reflect in the chemical potential μ, as in equilibrium gas flow can only occur along a gradient in μ, and a circular flow would not be possible.

A method to create *controlled* nonequilibrium conditions is to generate surface nanobubbles through electrolysis [11,46]. In Ref. [46] it has been shown that several tens of seconds after switching on the potential, these surface nanobubbles do not further grow, in spite of a nonzero current. This observation suggests that the nanobubbles indeed have achieved a *dynamic* stable equilibrium, with the Laplace pressure driven gas outflux being compensated by the gas influx at the electrode.

In summary, we have suggested a dynamic equilibrium stabilization mechanism for surface nanobubbles: The gas outflux driven by Laplace pressure is compensated by a gas influx at the contact line, leading to a metastable equilibrium under certain conditions. A necessary ingredient into this model is a contact angle decrease with decreasing bubble size R. Though such a decrease has been observed both experimentally [43,44] and numerically [39,40], further work is required to better quantify and understand this dependence $\theta(R)$.

[1] P. Ball, Nature (London) **423**, 25 (2003).
[2] O. Vinogradova et al., J. Colloid Interface Sci. **173**, 443 (1995).
[3] J. W. G. Tyrrell and P. Attard, Phys. Rev. Lett. **87**, 176104 (2001).
[4] P. Attard, Adv. Colloid Interface Sci. **104**, 75 (2003).
[5] M. Holmberg et al., Langmuir **19**, 10510 (2003).
[6] A. Simonsen, P. Hansen, and B. J. Klösgen, J. Colloid Interface Sci. **273**, 291 (2004).
[7] X. H. Zhang et al., Langmuir **20**, 3813 (2004).
[8] A. Agrawal et al., Nano Lett. **5**, 1751 (2005).
[9] C. Neto, D. R. Evans, E. Bonaccurso, H. J. Butt, and V. S. J. Craig, Rep. Prog. Phys. **68**, 2859 (2005).
[10] X. H. Zhang, N. Maeda, and V. S. J. Craig, Langmuir **22**, 5025 (2006).
[11] L. Zhang et al., Langmuir **22**, 8109 (2006).
[12] S. Yang, S. Dammer, N. Bremond, H. J. W. Zandvliet, E. S. Kooij, and D. Lohse, Langmuir **23**, 7072 (2007).
[13] B. M. Borkent, S. M. Dammer, H. Schönherr, G. J. Vancso, and D. Lohse, Phys. Rev. Lett. **98**, 204502 (2007).
[14] S. Yang, E. S. Kooij, B. Poelsema, D. Lohse, and H. J. W. Zandvliet, Europhys. Lett. **81**, 64 006 (2008).
[15] X. H. Zhang, A. Quinn, and W. A. Ducker, Langmuir **24**, 4756 (2008).
[16] X. H. Zhang, A. Khan, and W. A. Ducker, Phys. Rev. Lett. **98**, 136101 (2007).
[17] J. W. G. Tyrrell and P. Attard, Langmuir **18**, 160 (2002).
[18] X. H. Zhang et al., Langmuir **23**, 1778 (2007).
[19] M. Mezger et al., Proc. Natl. Acad. Sci. U.S.A. **103**, 18 401 (2006).
[20] A. Poynor et al., Phys. Rev. Lett. **97**, 266101 (2006).
[21] M. Mezger et al., J. Chem. Phys. **128**, 244705 (2008).
[22] M. Switkes and J. W. Ruberti, Appl. Phys. Lett. **84**, 4759 (2004).
[23] E. Lauga, M. P. Brenner, and H. A. Stone, in *Handbook of Experimental Fluid Dynamics*, edited by C. Tropea, J. Foss, and Y. A. (Springer, New York, 2005).
[24] T. H. Fan and O. I. Vinogradova, Phys. Rev. E **72**, 066306 (2005).
[25] O. I. Vinogradova and G. E. Yakubov, Phys. Rev. E **73**, 045302(R) (2006).
[26] P. S. Epstein and M. S. Plesset, J. Chem. Phys. **18**, 1505 (1950).
[27] P. G. de Gennes, F. Brochard-Wyart, and D. Quere, *Capillarity and Wetting Phenomena* (Springer, Berlin, 2003).
[28] K. Karraker and C. Radke, Adv. Colloid Interface Sci. **96**, 231 (2002).
[29] S. Ljunggren and J. C. Eriksson, Colloids Surf. A **130**, 151 (1997).
[30] C. Fradin et al., Nature (London) **403**, 871 (2000).
[31] S. Mora et al., Phys. Rev. Lett. **90**, 216101 (2003).
[32] F. Jin, J. Li, X. Ye, and Chi Wu, J. Phys. Chem. B **111**, 11 745 (2007).
[33] E. Dressaire et al., Science **320**, 1198 (2008).
[34] B. D. Johnson and R. C. Cooke, Science **213**, 209 (1981).
[35] S. Dammer and D. Lohse, Phys. Rev. Lett. **96**, 206101 (2006).
[36] A. Luzar and D. Bratko, J. Phys. Chem. B **109**, 22 545 (2005).
[37] D. Bratko and A. Luzar, Langmuir **24**, 1247 (2008).
[38] R. Steitz et al., Langmuir **19**, 2409 (2003).
[39] A. Checco, P. Guenoun, and J. Daillant, Phys. Rev. Lett. **91**, 186101 (2003).
[40] A. Checco, H. Schollmeyer, J. Daillant, P. Guenoun, and E. Boukherroub, Langmuir **22**, 116 (2006).
[41] P. Jakubczyk and M. Napiorkowski, J. Phys. Condens. Matter **16**, 6917 (2004).
[42] D. Li, Colloids Surface A: Physicochem. Eng **116**, 1 (1996).
[43] N. Kameda and S. Nakabayashi, Chem. Phys. Lett. **461**, 122 (2008).
[44] N. Kameda and S. Nakabayashi, Surf. Sci. **602**, 1579 (2008).
[45] J. Gaydos and A. W. Neumann, J. Colloid Interface Sci. **120**, 76 (1987).
[46] S. Yang, P. Tasi, E. S. Kooij, A. Prosperetti, H. J. W. Zandvliet, and D. Lohse, Langmuir (to be published).